

Evaluation of Well Performance for the Slot-Drill Completion in Low- and Ultralow-Permeability Oil and Gas Reservoirs

T.O. Odunowo, DeGolyer & MacNaughton/Texas A&M University; G.J. Moridis, SPE, Lawrence Berkeley National Laboratory/Texas A&M University; T.A. Blasingame, SPE, Texas A&M University; O.M. Olorode, Afren Resources/Texas A&M University; C.M. Freeman*, Texas A&M University

Summary

Low- to ultralow-permeability formations require “special” treatments/stimulation to make them produce economical quantities of hydrocarbon, and at the moment, multistage hydraulic fracturing (MSHF) is the most commonly used stimulation method for enhancing the exploitation of these reservoirs. Recently, the slot-drill (SD) completion technique was proposed as an alternative treatment method in such formations (Carter 2009).

This paper documents the results of a comprehensive numerical-simulation study conducted to evaluate the production performance of the SD technique and compare its performance to that of the standard MSHF approach. We investigated three low-permeability formations of interest—namely, a shale-gas formation, a tight-gas formation, and a tight/shale-oil formation. The simulation domains were discretized with Voronoi-gridding schemes to create representative meshes of the different reservoir and completion systems modeled in this study.

The results from this study indicated that the SD method does not, in general, appear to be competitive in terms of reservoir performance and recovery compared with the more traditional MSHF method. Our findings indicate that the larger surface area to flow that results from the application of MSHF is much more significant than the higher conductivity achieved by use of the SD technique. However, there may exist cases, for example, a lack of adequate water volumes for hydraulic fracturing, or very high irreducible water saturation that leads to adverse relative permeability conditions and production performance, in which the low-cost SD method may make production feasible from an otherwise challenging (if not inaccessible) resource.

Introduction

Shale-gas and other low-/ultralow-permeability hydrocarbon reservoirs have recently emerged as very important energy sources. Such reservoirs, which are often referred to as “unconventional” resources, have now become the hub of exploration-and-production (E&P) activities in several areas, but mainly in North America. As of 2005, more than 25% of the daily natural-gas production in the US was derived from unconventional reservoirs (Naik 2005). The SD method is a completion technique that can be used to recover hydrocarbons from such low-permeability reservoirs.

The SD-Completion Method. The proposed SD technique is an advanced cable-saw method that works like a “downhole hacksaw,” and is suitable for application at depths ranging from 1,000 to 10,000 ft (Carter 2009). It involves the use of a tensioned abrasive cable, which is attached to the drillpipe, to create a slot

perpendicular to the wellbore up to 100 ft deep into the target formation (Fig. 1). The SD is purported to provide a large surface area and a high-conductivity conduit in the low-permeability formation, thus enhancing hydrocarbon flow and production.

To create the SD completion in a target formation, the following process is followed. First, the well is drilled (to a predetermined kickoff depth in the target formation) and cased. This kickoff depth is usually a few feet into the target formation to ensure that the slot is formed within it. Next, the horizontal section of the well is drilled, but with the tip pointing upward in a mirrored J-like manner (as illustrated in Fig. 1). The drillstring is then retrieved, and the cutting abrasive cable is attached to its tip with a special downhole shoe-joint tool. The cable is a 1.5-in.-diameter steel-wire rope (Fig. 1).

On the rig, an automatic tension-regulating winch maintains a specific tension on the cable as the drillstring assembly is lowered back into the hole. This tension prevents the pipe from turning and wrapping up the cable on its way back down. It also makes the abrasive cable “cling” to the inner radius of the curved wellbore, whereas the compressive forces (on the drillpipe) push the drillpipe against the outer radius. The reciprocating “up and down” motion of this assemblage is the driving force on the “saw” to create the slot in the formation. The resulting cutting force at any point is a function of the local cable tension and the radius of curvature. This process is expected to yield a crescent-shaped slot, the thickness of which is controlled by the diameter of the cutting cable (1.5 in. in this study, as initially proposed by Carter 2009).

The potential advantages of the SD completion over MSHF include

- The elimination of the massive volumes of water required for hydraulic fracturing. This makes the SD a more environmentally friendly completion than MSHF.
- Significant control over the resulting fracture (slot) geometry and penetration.
- The creation of slots in the reservoir of approximately 1.5 in., which have significantly higher conductivities (k_{app}) than typical hydraulic-fracture conductivities.
- The lower cost of implementing this method (approximately half the cost of a hydraulic-fracturing job).

However, the most important question to be asked is how well the SD would perform, in terms of production enhancement, in the applicable formations of interest. This numerical-simulation study aims to address this question.

Geology of the Selected Formations. This study evaluated the performance of the SD method in shale-gas formations, tight-gas formations, and tight/shale-oil formations. The reservoir properties used in the simulation of each of these three systems were obtained from representative average properties of (a) the Cotton Valley (a tight gas formation), (b) the Marcellus (a shale-gas formation), and (c) the Bakken (a tight/shale-oil formation).

The Upper Jurassic and Lower Cretaceous Cotton Valley Group is an extensive, coastal strand-plain sandstone deposition

* Now with Hilcorp Energy Company.

Copyright © 2014 Society of Petroleum Engineers

This paper (SPE 164547) was accepted for presentation at the Unconventional Resources Conference USA, The Woodlands, Texas, USA, 10–12 April 2013, and revised for publication. Original manuscript received for review 25 January 2013. Revised manuscript received for review 3 November 2013. Paper peer approved 25 November 2013.

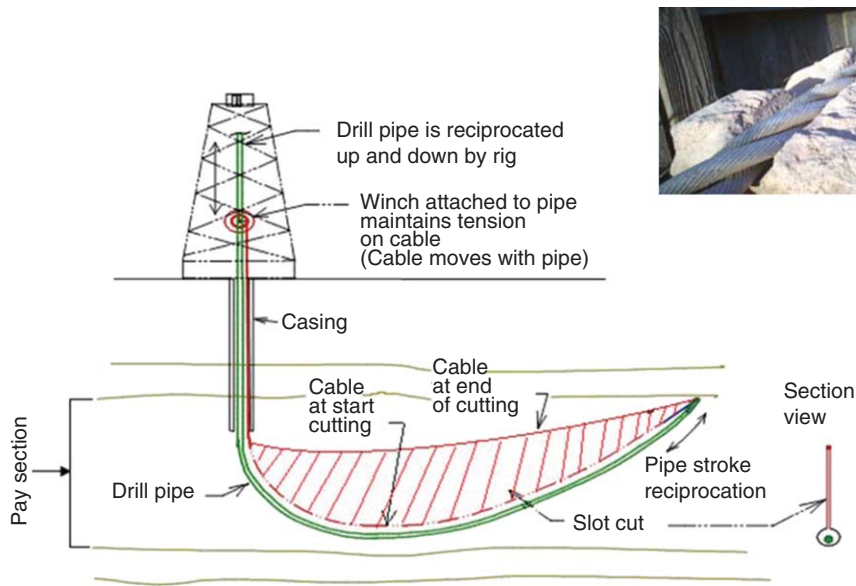


Fig. 1—Schematic of the SD completion with an insert illustrating how the steel-wire rope cuts through the formation matrix (used with permission from Carter 2009).

TABLE 1—GENERAL MODEL PARAMETERS

Parameters	SI Units	Field Units
Fracture half-length, x_f	100.0 m	328.1 ft
Fracture width, w_f	3.0 mm	0.1 in.
Slot width, w_{slot}	12.7 mm	0.5 in.
Fracture spacing, d_f	108.9 m	357.1 ft
Well length, L_w	762.0 m	2,500.0 ft
Number of fractures	7	7
Fracture permeability, k_{frac}	$5.0 \times 10^{-11} \text{ m}^2$	$5.1 \times 10^4 \text{ md}$
Slot permeability, k_{slot}	$1.0 \times 10^{-10} \text{ m}^2$	$1.0 \times 10^5 \text{ md}$
Fracture porosity, ϕ_{frac}	0.33	0.33
Well radius, r_w	0.1 m	0.3 ft
Well pressure, p_{wf}	$3.5 \times 10^6 \text{ Pa}$	500.0 psia

TABLE 2—REPRESENTATIVE COTTON VALLEY TIGHT-GAS-FORMATION PARAMETERS

Parameters	SI Units	Field Units
Reservoir thickness, h	45.7 m	150.0 ft
Reservoir width, w	304.8 m	1,000.0 ft
Permeability, k_{sand}	$5.9 \times 10^{-18} \text{ m}^2$	$6.0 \times 10^{-3} \text{ md}$
Matrix porosity, ϕ	0.08	0.08
Temperature, T	119.4 °C	247.0 °F
Reservoir pressure, p_i	$28.6 \times 10^6 \text{ Pa}$	4,154 psia

in eastern Texas and in northwestern Louisiana that overlies the Haynesville/Bossier shale. Although it is composed of laminated shale, sandstone, and limestone deposits (Dyman and Condon 2006), the average parameters used for this study were obtained only from the productive sandstone formation.

The Marcellus shale is one of the main shale-gas plays of North America in terms of total gas resource, extent, production rates, and economic potential. In the US, it covers regions in New York, northern and western Pennsylvania, eastern Ohio, western Maryland, and most of West Virginia. The organic-rich shale of the Marcellus was deposited in a foreland basin setting that was sediment starved and allowed for accumulation and preservation of the organic material (Zagorski et al. 2011). The Marcellus shale

formation occurs in the lower part of the Hamilton group, which is bounded above by the Middle Devonian Tully limestone and below by the Lower Devonian Onondaga limestone. The Upper and Lower Marcellus shale are separated by the Cherry Valley/Purcell limestone.

The Bakken formation is a rock unit from the Late Devonian to Early Mississippian that occupies approximately 200,000 sq miles (520 000 km²) of the subsurface of the Williston basin. It covers parts of Montana, North Dakota, and Saskatchewan. It is divided into three rock units or members that are composed of the 18-ft-thick upper member, the 41-ft-thick middle member, and the 19-ft-thick lower member (Boleneus 2010). Both the upper and lower members contain a high percentage of organic carbon and are classified by some investigators as oil shales. The middle member is an argillaceous dolomite and has proved to be the most productive of the three so far; thus, this is where recent industry activity has focused (Flannery and Kraus 2006). Oil was first discovered within the Bakken in 1951 (Heck et al. 2012).

TABLE 3—REPRESENTATIVE MARCELLUS SHALE-GAS PARAMETERS

Parameters	SI Units	Field Units
Reservoir thickness, h	45.7 m	150.0 ft
Reservoir width, w	304.8 m	1,000.0 ft
Permeability, k_{shale}	$7.4 \times 10^{-20} \text{ m}^2$	$7.5 \times 10^{-5} \text{ md}$
Matrix porosity, ϕ	0.09	0.09
Temperature, T	51.7 °C	125.0 °F
Reservoir pressure, p_i	$24.1 \times 10^6 \text{ Pa}$	3,500 psia

Model Parameters and Setup. The general petrophysical, completion, and other reservoir parameters used for all the simulations conducted in this study are presented in Table 1. The properties that vary in the different selected formations are shown in Tables 2 through 4. The values in these tables were extracted from the works of Soeder (1988), Boleneus (2010), and Bartberger et al. (2002), and the Ground Water Protection Council's (GWPC) shale-gas primer report for the US Department of Energy (US Department of Energy 2009), publications by Halliburton on unconventional resources (Halliburton 2008a, b), and the Gas Technology Institute (GTI) map on tight gas resources in the US (GTI 2001).

TABLE 4—REPRESENTATIVE BAKKEN TIGHT/SHALE-OIL PARAMETERS

Parameters	SI Units	Field Units
Reservoir thickness, h	12.5 m	41.0 ft
Reservoir width, w	1219.2 m	4,000.0 ft
Permeability, k_{sand}	$2.0 \times 10^{-17} \text{ m}^2$	$2.0 \times 10^{-2} \text{ md}$
Matrix porosity, ϕ	0.07	0.07
Temperature, T	76.7°C	170.0°F
Reservoir pressure, p_i	$32.1 \times 10^6 \text{ Pa}$	4,653 psia

Domain Discretization. The spatial discretization of the reservoir-simulation domain was performed with unstructured (Voronoi) grids. These grids have the advantage of being flexible because they can assume any shape, size, or orientation. The SD completion has the shape of an arc segment, and as a result of its high-conductivity, curvilinear flow patterns are expected around its tips and edges. As a result, developing a Cartesian system to accurately represent this configuration would have required a very fine discretization, resulting in an inordinately large number of gridblocks.

For each target formation we considered, we developed grids for six reservoir/completion configurations. The mesh generation was a three-step process. First, we generated an array of gridblock centers that was necessary to create a grid representative of the desired configuration. These centers were then imported into the “vorop++” application (Rycroft 2007) to provide the Voronoi tessellations that yielded the unstructured grids. Finally, we used an adaptation of TAMMESH (Olorode 2011) for further post-processing of the output from “vorop++”. A detailed discussion of this gridding process is beyond the scope of this paper; the interested reader is referred to Odonowo (2012). All the grids were visualized with “Gnuplot,” a public-domain UNIX visualization software package (<http://www.gnuplot.info/>).

The first configuration (Geometry A) was that of a horizontal well in the reservoir with no stimulation. This served as the base (reference) case against which the different stimulation options were compared, to assess the relative performance of the various configurations. The second configuration (Geometry B) involved a curved well in the reservoir and represented an unstimulated case (i.e., there was no hydraulic fracturing following the installation of the curved well). This configuration was useful in assessing if the extra well length resulting from the curvature of the well in the SD method provides a production advantage over a straight-horizontal-well case.

The attempt to model the SD completion resulted in two grid systems—one in which the SD completion was represented with a “close-to-actual” geometry (arc-segment shape) and another one in which an approximate (rectangular) representation of its geometry was used (Geometries C and D, respectively). The slot’s surface area in this “equivalent SD (ESD) representation” was kept the same as in the “close-to-actual” representation. The fifth configuration (Geometry E) was that of a case when the reservoir was completed with MSHF. The final stimulated case (Geometry F) represented a hypothetical scenario that involved a combination of the SD completion with MSHF. Visualizations of these different grid meshes that were used for this study are also presented in the Odonowo (2012) reference.

Numerical Simulation of Reservoir Performance. We used the TAMSIM code (Freeman 2010) for the simulations in this study. TAMSIM is a fully implicit, nonisothermal, multidimensional numerical simulator developed at Texas A&M University on the basis of the TOUGH+ simulator (Moridis et al. 2010), for the analysis of flow and transport in unconventional gas and oil reservoirs.

Stencils were used to reduce the dimensionality of the problem and, consequently, the execution time required for the simula-

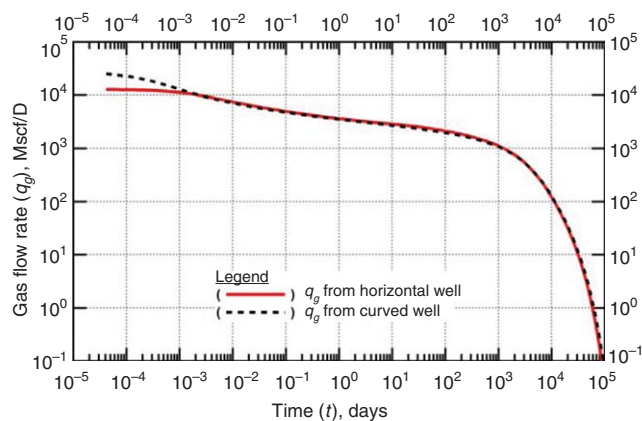


Fig. 2—Tight-gas-reservoir simulation results: Rate profile of the curved-well system (Geometry A) matches that of the straight horizontal-well system (Geometry B).

tions. A stencil is the smallest (minimal) repeatable subdomain (division or segment of the entire domain) that can provide a sufficiently representative solution to characterize the flow in the domain under study. To obtain the rates and cumulative production values for the full grid, the stencil rates and cumulative production values were simply multiplied by the number of times the stencil occurs in the full grid. This concept is discussed extensively by Freeman (2010).

Equivalency Studies

In these studies, production estimates from two configuration sets were compared to determine their degree of agreement. These sets were (a) the straight-well and the curved-well case and (b) the “close-to-actual” and ESD representations of the SD completion.

Straight-Well vs. Curved-Well Production. The SD completion method involves drilling a well with a curved trajectory. This results in a longer well length than that of a straight well and, consequently, in a larger surface area available for fluid flow from the formation. The length of the straight horizontal well in the systems we considered was 2,500 ft, whereas the curvature of the curved well resulted in an extra well length of slightly more than 15 ft. Thus, we investigated if this extra well length would result in an advantage for the SD completion (in terms of overall gas production) over other completion methods. To that end, we compared the production rates from the straight well with those from the curved-well cases in all three of the target formations of interest.

Fig. 2 shows a comparison of the production rates from the curved well and from the straight horizontal well in the tight-gas-formation study. The rates from both well geometries practically coincided after a very short initial period, indicating that there was practically no advantage of the curving (and longer) well over the straight well in the tight gas formation used in this study. The slight deviation between the two curves at very early times (less than 0.001 days) was attributed to the different initial well-bore drainage (a plausible physical reason), but results at this time can be affected by numerical artifacts and discretization errors that are mitigated as time advances. As a result of the close match, no production advantage needed to be taken into account when the straight well was used as the (unstimulated) reference case in the evaluation of production from the stimulated systems.

Fig. 3 displays the results of this study in the shale-gas reservoir. Here also, the agreement between the two solutions was excellent after an initial very early-stage separation. This deviation was ascribed to early-time numerical-discretization errors and could be ignored for practical purposes. Thus, the extra length of the curving well appears to offer no advantage over the case of

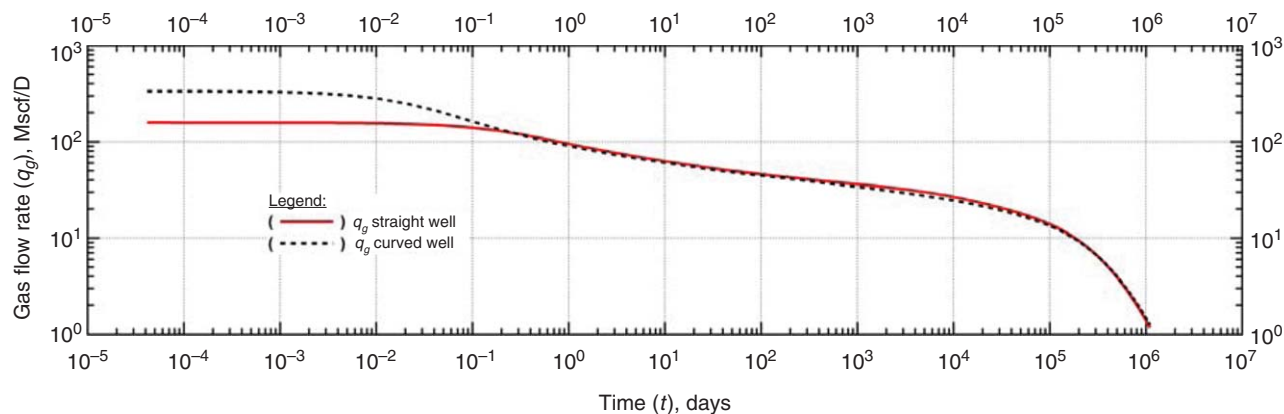


Fig. 3—Shale-gas-reservoir simulation results: Rate profile of the curved-well system (Geometry A) matches that of the straight horizontal-well system (Geometry B).

the straight horizontal well during production from the shale-gas system used in this study.

We reached the same conclusions in the tight/shale-oil case. Though not as near-perfect as in the previous cases, we observed a good overall match (Fig. 4), leading to the conclusion that the longer length of the curving well does not provide any production advantage. The less-than-perfect match observed was ascribed to gravity effects that are more significant in this case (oil being denser than gas).

The “Close-to-Actual” SD vs. the ESD Representation. The SD geometry is rather complex and tedious to model and analyze. To avoid unnecessarily complex, demanding, and time-consuming work in future studies, we investigated the possibility of using a simpler (approximate) grid configuration that could predict production from the SD completion with an acceptable level of accuracy. This was performed by comparing the production rates from the “close-to-actual” and ESD representations of the SD completion.

Fig. 5 shows the results of this study in the tight gas reservoir. Production rates from both grid configurations match almost perfectly, thus validating the hypothesis that an appropriately designed ESD representation can accurately estimate the production performance of a SD completion described by a complex 3D grid geometry in the tight gas reservoir we studied. The spatial pressure distributions, shown in Figs. 6 and 7, also indicate a similarity in the depletion of both reservoir systems over time. As expected, production from the SD completion exhibits a linear-flow signature (one-half slope on the log-log plot in Fig. 5) before

the pressure transient reaches the boundaries, after which a more rapid decline occurs.

Fig. 8 shows the production estimates from the ESD and the fully described SD representation in the shale-gas study. Apart from a slight deviation at very early times (less than 0.01 days), a near-perfect match is observed. The early deviation was attributed to early-time differences in the wellbore drainage in the two models caused by their different well trajectories (curved as opposed to straight); this difference is more visible in the shale-gas study as opposed to the tight-gas-formation study because of a much higher completion/formation permeability contrast. However, the observed match is satisfactory and validated the hypothesis that the simpler ESD configuration could accurately represent the full-SD completion. The overall pressure response to production in the shale-gas systems was very similar to that of the tight gas systems shown in Figs. 6 and 7. The only difference was that it took longer for the pressure transient to permeate the shale-gas systems (as a result of the lower formation permeability). This parallel similarity was replicated in all the other studies, and, as such, the spatial pressure-distribution plots corresponding to the shale-gas systems are omitted in this paper.

The same trend persists in the tight/shale-oil study. Fig. 9 shows a near-perfect match between the production-rate estimates in the two cases, thus validating the hypothesis that provided the impetus for this study. Likewise, reservoir-pressure maps (Fig. 10) of both cases also show identical reservoir depletion with time. In this case, and in the case of the other tight/shale-oil studies, only the plan view of the reservoir is displayed. The

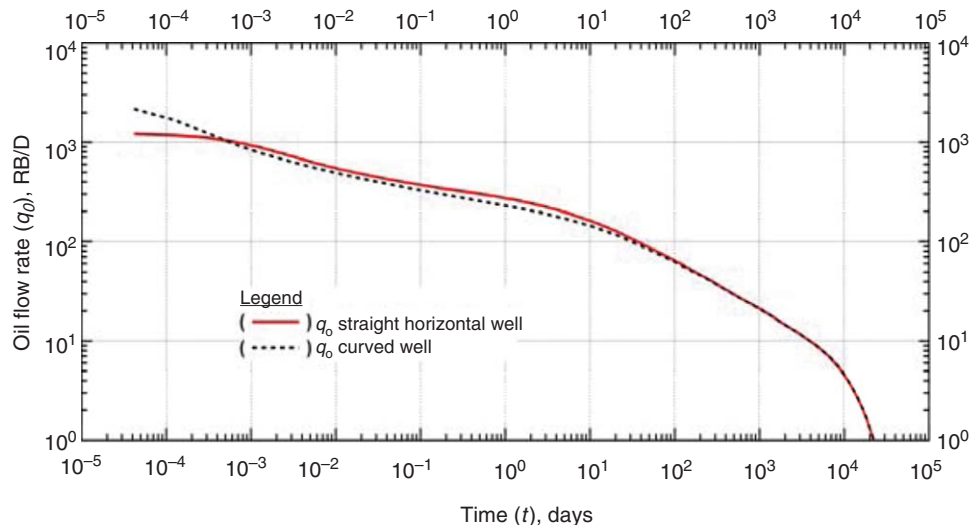


Fig. 4—Tight-shale-oil-reservoir simulation results: Rate and cumulative-production plots illustrating the near-equivalent production signature of the curved-well system (Geometry A) and the straight horizontal-well system (Geometry B).

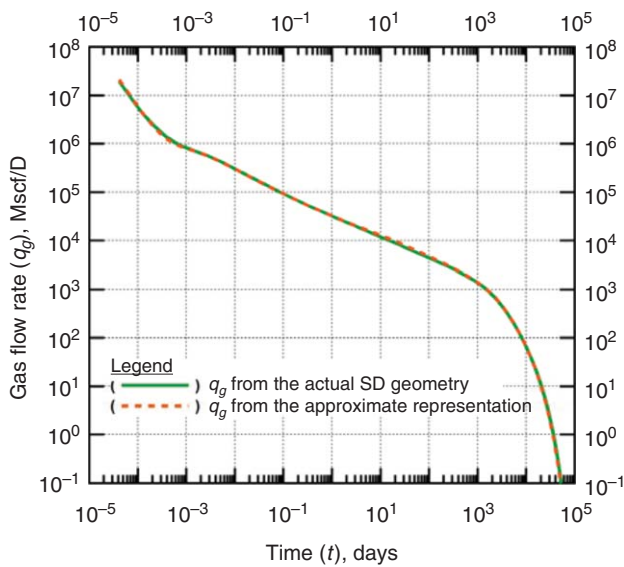


Fig. 5—Tight-gas-reservoir simulation results: Production rates from the ESD representation (Geometry D) match those from the “close-to-actual” representation (Geometry C).

productive zone of the Bakken formation is thin and extensive (see Table 4)—resulting in a sheet-like geometry for the tight/shale-oil reservoir we simulated. Therefore, presenting 3D views of the formation would provide no additional (to what could be seen in the plan views) information in this case.

Comparative Studies

In this part of the study, we compared the production performance of the SD completion with that corresponding to an MSHF treat-

ment. We also compared the performance of the hypothetical combination of the MSHF with the SD completion to that of the standard MSHF treatment to determine whether such a combination could lead to a significant boost in production. The plots showing these comparisons include the production-rate curve from the straight-horizontal-well (unstimulated) system as a reference.

The SD Completion vs. MSHF. Fig. 11 shows the production rates from the tight gas reservoirs completed with these two stimulation methods. Production rates are higher for the MSHF case during the most important production period (i.e., from approximately 0.01 days to almost 1,000 days), although they become lower than those for the SD completion for $t > 1,000$ days. A more thorough evaluation of the relative performance in the two cases emerges after a comparison of the cumulative production from the two stimulation methods, shown in Fig. 12. The consistent advantage of the MSHF treatment during a period of 30 years (a reasonable approximation for the producing life of the tight gas reservoir) is obvious, especially if the production period is short; on the other hand, the advantage shrinks continuously with time if production is maintained for a very long period. Fig. 12 clearly indicates that the performance of the SD completion is a significant improvement over that in the unstimulated case (the straight horizontal well), but the MSHF treatment offers a consistent advantage. It appears that the larger surface area to flow that MSHF provides (1.378×10^6 ft² for MSHF as opposed to 0.401×10^6 ft² for the SD method) is much more significant than the higher conductivity (4,208 md-ft for the SD method as opposed to 499 md-ft for MSHF) achieved with the SD technique. Fig. 13 shows the evolution of the reservoir-pressure distribution in the MSHF-completed reservoir at different times through production. This figure also shows a faster pressure depletion, as a result of higher production, in the MSHF reservoir than in the SD-completed reservoir (Fig. 6).

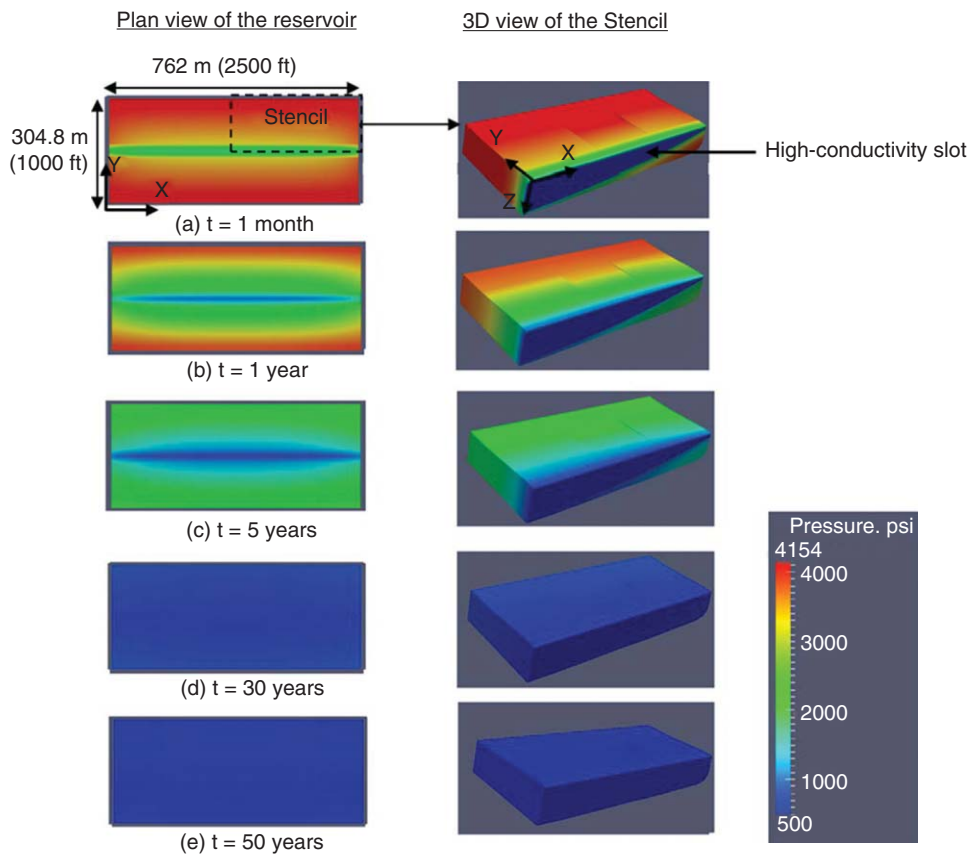


Fig. 6—Plan views of the full reservoir and 3D views of the stencil showing the spatial distribution of pressure in the tight gas reservoir corresponding to Fig. 5, at various stages of production when producing from the SD completion (Geometry C).

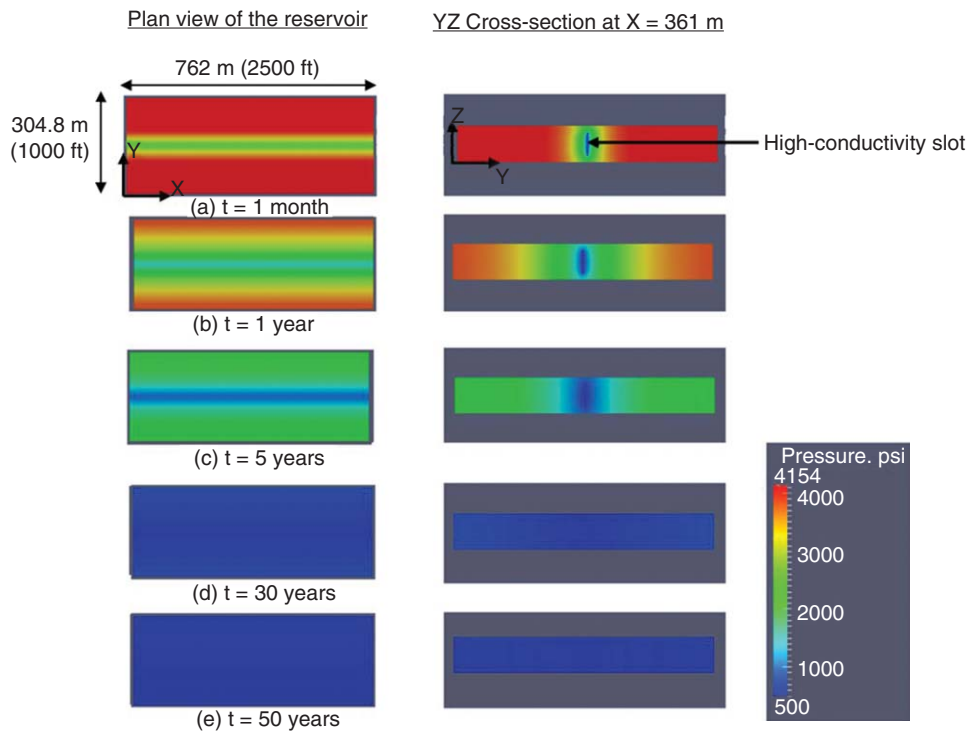


Fig. 7—Plan views and cross-sectional views of the spatial distribution of pressure in the tight gas reservoir corresponding to Fig. 5, at various stages of production from the ESD representation (Geometry D).

A similar picture emerges in the shale-gas study. As shown in Fig. 14, the production rates from the SD-completed reservoir generally did not compare favorably with the rates from the MSHF treatment. The curves in the cumulative-production plot (Fig. 15) make this even more obvious. A longer reservoir life (100 years) was assumed here because of the lower permeability of the shale-gas formation (compared with the tight gas formation). The observed results here also led to a similar conclusion that the larger surface area to flow created by MSHF was more significant to production enhancement than the higher conductivity achieved from the SD technique. The surface area and fracture/slot conductivities here have the same values in the tight-gas-formation case.

Fig. 16 shows clearly that, for practically all the important part of the life of the tight/shale-oil reservoir (with the exception of a very early short period with unimportant impact in the overall behavior), the production rates from the SD-completed reservoir

generally did not compare favorably with the rates from the MSHF-completed reservoir. From the cumulative-production curves in Fig. 17, the MSHF system is shown to consistently outperform the SD completion. In the case of the tight/shale-oil study, MSHF resulted in a fracture conductivity of 499 md-ft and an overall surface area of 0.377×10^6 ft², whereas the SD technique resulted in a slot conductivity of 4,208 md-ft but an overall surface area of 0.126×10^6 ft². This reinforces the earlier assertion that the surface area available to flow is a more significant factor, in terms of production performance, than the conductivity of the slot or fracture.

However, it is important to note that, although MSHF has a consistent advantage, the production performance of the SD technique can still be deemed acceptable (and possibly satisfactory) under certain conditions, especially when its lower cost (compared with that of MSHF) is considered. Thus, the advantage (and appeal) of the MSHF treatment may be reduced (or even eliminated) in cases, for example, in which standard hydraulic fracturing may be hampered for lack of appropriate volumes of water,

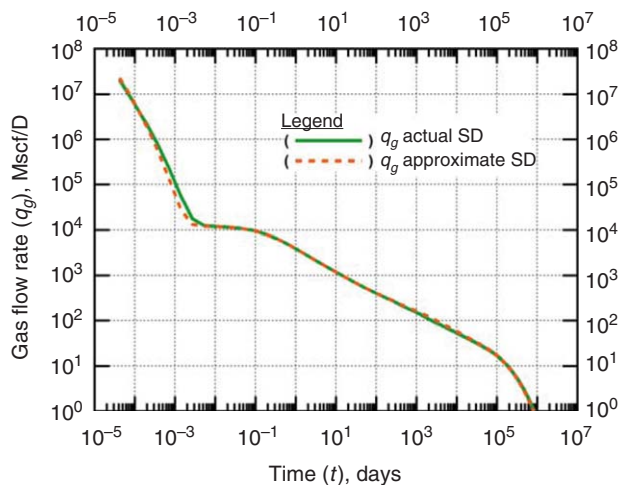


Fig. 8—Shale-gas-reservoir simulation results: Production rates from the ESD representation (Geometry D) match those from the “close-to-actual” representation (Geometry C).

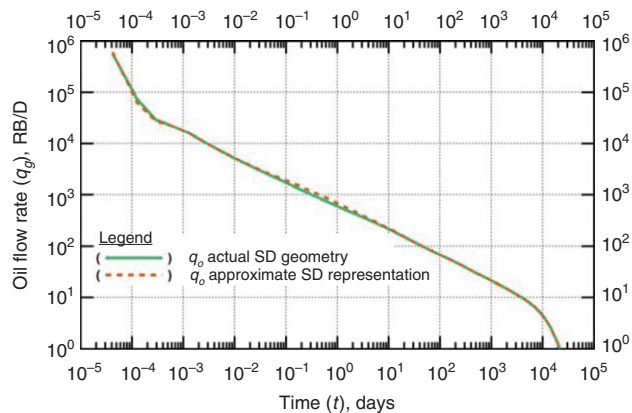


Fig. 9—Tight/shale-oil-reservoir simulation results: Rate profile from the ESD representation (Geometry D) matches that of the “close-to-actual” SD representation (Geometry C).

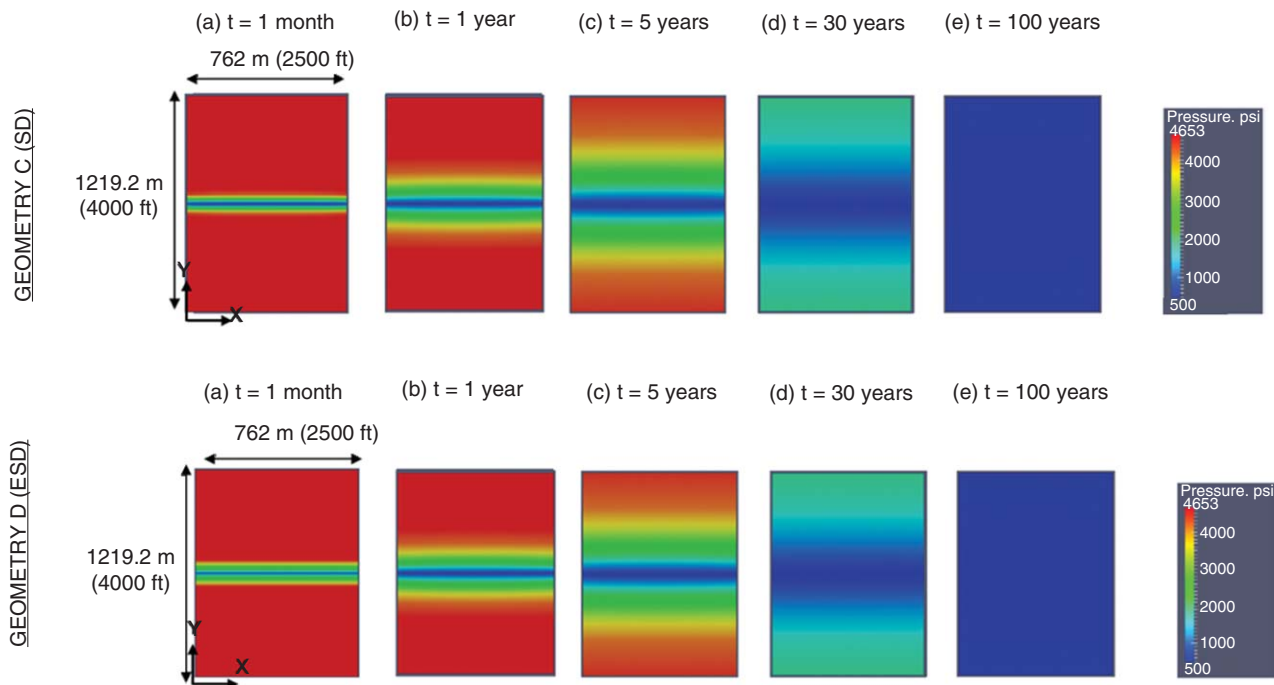


Fig. 10—Plan views of the pressure distribution over time in the tight oil reservoir corresponding to Fig. 9, during oil production from the SD and ESD configurations (Geometry C and D).

when the irreducible water saturation of the formation is very high (leading to an adverse relative permeability regime of the escaping gas and, consequently, low production), and when the formation is strongly affected by gels often used in the fracturing liquids. Thus, it is possible that the SD technique may render production feasible from otherwise uninviting production targets.

MSHF vs. the Combination of the SD Method With MSHF.

Fig. 18. shows the production rates obtained from simulating both of these completion scenarios in the tight-gas-formation system. The initial production rates of the combination case are clearly higher, but the period over which this advantage exists is limited (less than 100 days). Similarly, the cumulative-production plot (Fig. 19) shows that the time period over which the production performance of the combination case dominated is short-

lived. Although there was some improvement in production, it was concluded that without a full economic analysis, it would not be possible to determine whether this improvement is sufficient to justify the extra expense of adding the SD completion.

For the shale-gas study, no significant boost in production over the standard MSHF system was achieved. The rate enhancement (as can be seen in Fig. 20) was only marginal, and limited to very early times (too short to make any practical difference). The cumulative-production plots in Fig. 21, however, showed a more significant improvement in the production performance of the combination case over the standard MSHF treatment case than what was observed in the tight-gas-formation study. As before, a full economic analysis would be required to determine whether the production boost is sufficient to justify the extra expense of adding the SD.

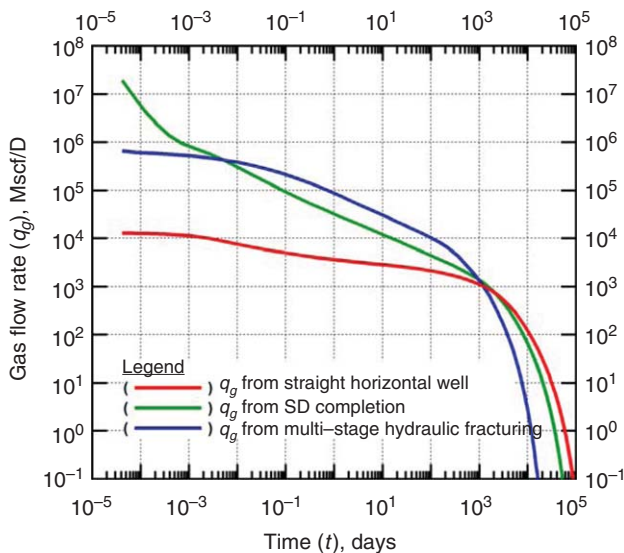


Fig. 11—Tight-gas-reservoir simulation results: Production rates from the SD completion were lower than those from the MSHF case during the linear-flow regime.

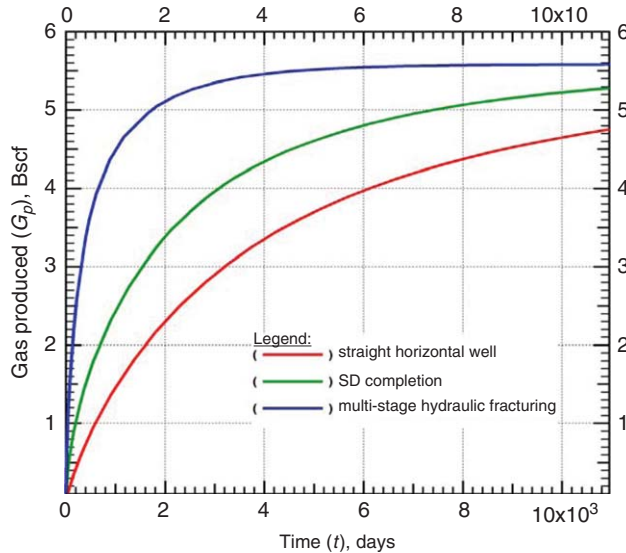


Fig. 12—Cumulative-production curves show that MSHF completion outperforms the SD completion in the tight-gas-formation study conducted.

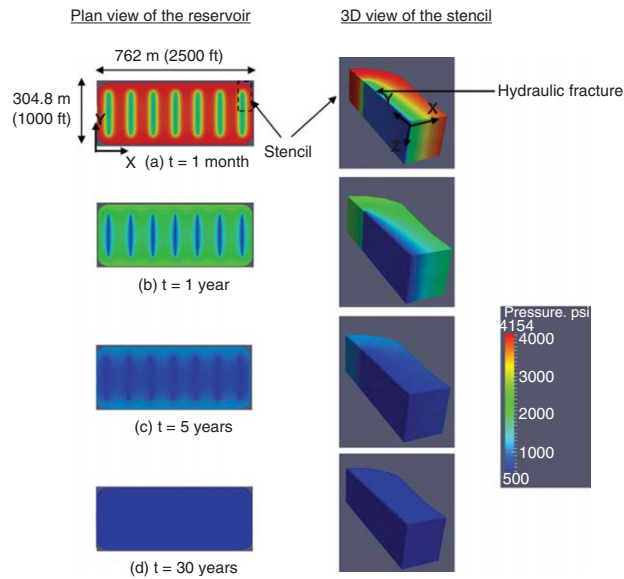


Fig. 13—Plan views of the full reservoir and 3D views of the stencil showing the spatial distribution of pressure in the tight gas reservoir corresponding to Fig. 12, at various stages of production when completed with MSHF (Geometry E).

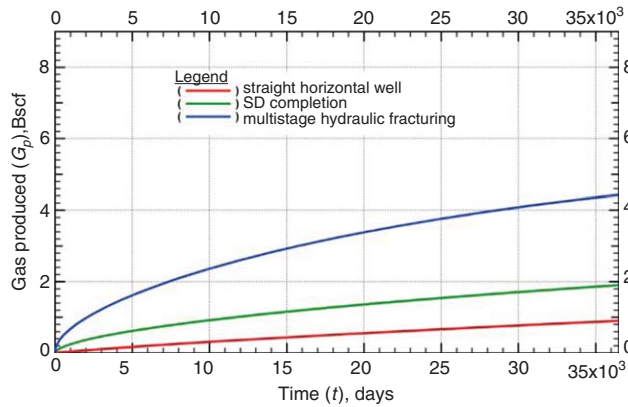


Fig. 15—Cumulative-production curves show that the SD completion fails to match up to the production enhancement obtained from MSHF in the shale-gas study conducted.

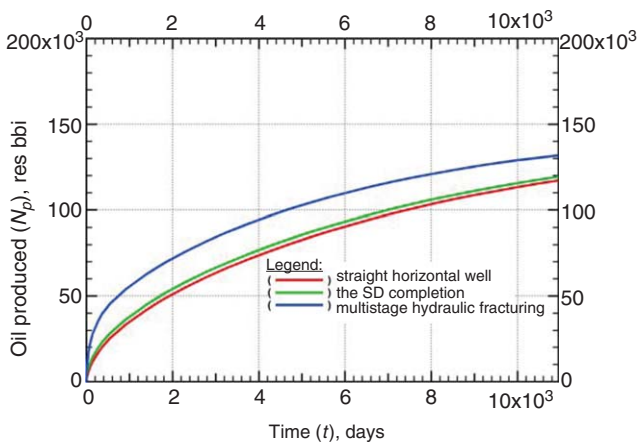


Fig. 17—Cumulative-production curves show that the improvement obtained from the implementation of the SD completion over the unstimulated-reservoir case is only marginal and does not match the improvement achieved from the MSHF.

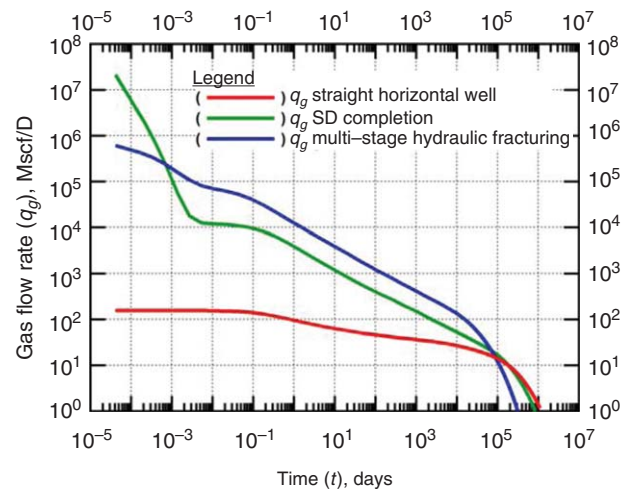


Fig. 14—Shale-gas-reservoir simulation results: Production from the SD completion did not match up favorably with those from the MSHF.

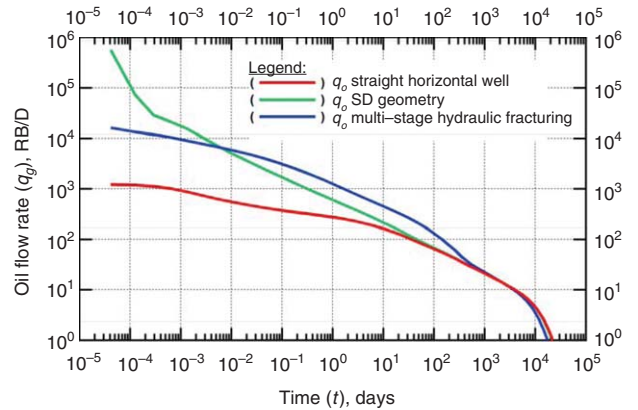


Fig. 16—Tight/shale-oil-reservoir simulation results: MSHF yields higher production rates than those from the SD completion during the fracture/slot linear-flow regime of the life of the tight/shale-oil reservoir.

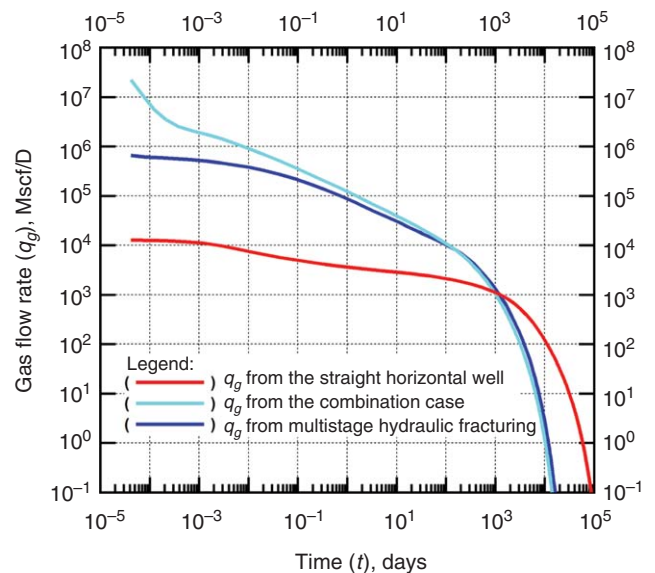


Fig. 18—Tight-gas-reservoir simulation results: Improvement in production rates obtained from the combination case over those from the MSHF appears to be only marginal and short-lived.

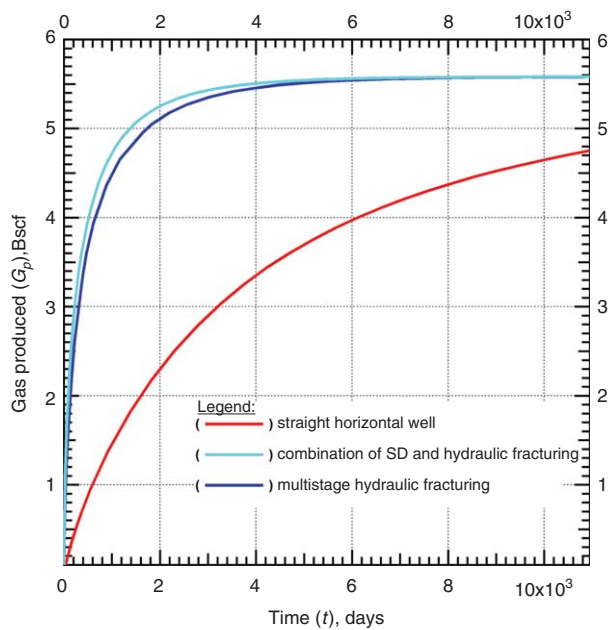


Fig. 19—Cumulative-production curves also show that the production advantage resulting from the combination of the SD method with MSHF in the tight-gas-formation study is only marginal.

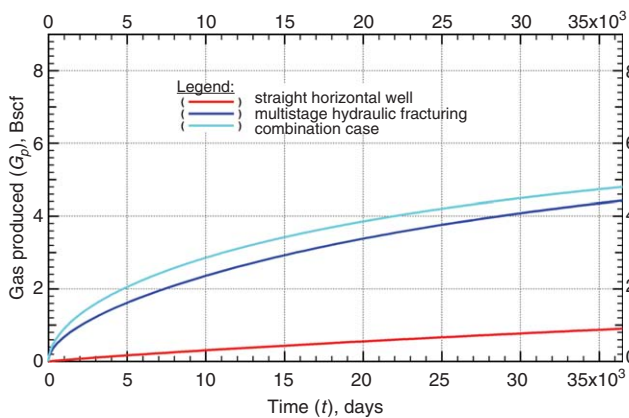


Fig. 21—Cumulative-production curves show some improvement in production rates resulting from the combination of the SD with MSHF in the shale-gas study.

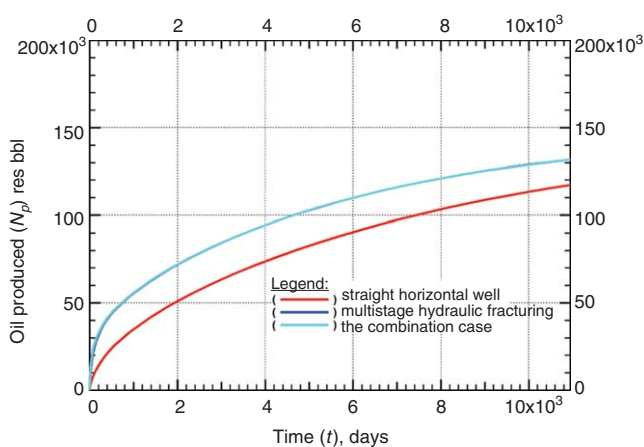


Fig. 23—Cumulative-production curves show that there is no noticeable production advantage resulting from the combination of the SD method with MSHF in the tight/shale-oil study.

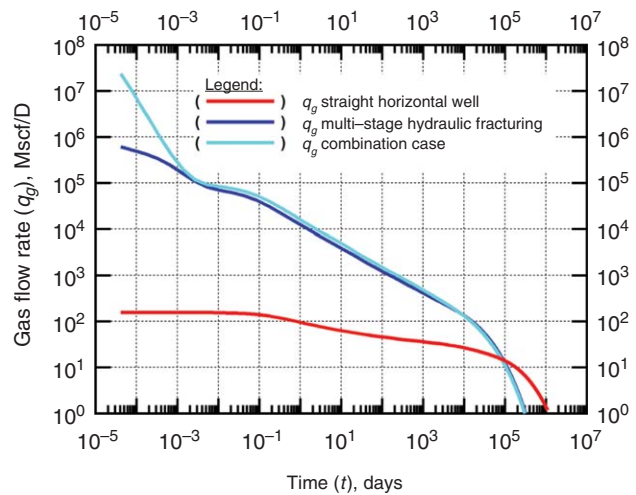


Fig. 20—Shale-gas-reservoir simulation results: Slight improvement in production rates is obtained when the SD is combined with MSHF.

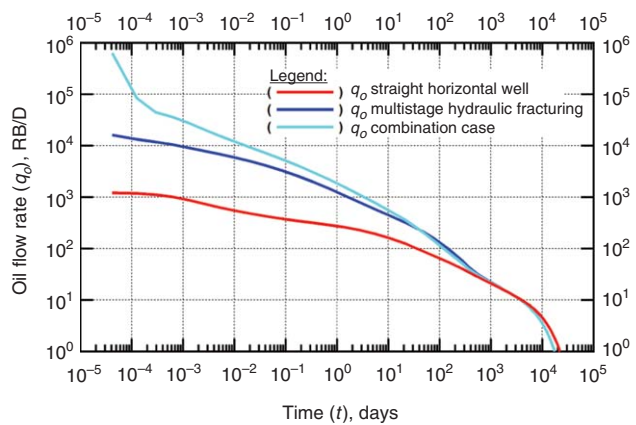


Fig. 22—Tight/shale-oil-reservoir simulation results: Production from the combination case shows only a short-lived (less than 10 days) slight improvement in production rates over the MSHF case.

Fig. 22 shows a plot of the obtained simulated production rates from the tight/shale-oil-reservoir systems with the two completion methods. Although there was some increase in the production rates in the combination case, this was a short-lived advantage (i.e., lasting approximately 10 days). The cumulative-production curves in Fig. 23 show that these early higher rates had a negligible overall effect.

Sensitivity Studies

In these studies, we investigated the impact of three parameters on the simulation results and conclusions reached in the preceding studies. These three parameters are

- The slot permeability (for the SD completion)
- The formation permeability
- The fracture conductivity/permeability (for the MSHF completion)

Sensitivity to the Slot Permeability. In this sensitivity study, we used the shale-gas-reservoir parameters, and we varied the slot permeability in the simulations with the two higher values listed in Table 5. As can be observed from Fig. 24, the higher slot permeability had practically no effect on the production rates for any reasonable timeframe. This is because the slot permeability at

Parameters	SI Units	Field Units
Slot permeability (higher), k_{slot}	$1.0 \times 10^{-9} \text{ m}^2$	$1.01 \times 10^6 \text{ md}$
Slot permeability (highest), k_{slot}	$1.0 \times 10^{-8} \text{ m}^2$	$1.01 \times 10^7 \text{ md}$

Parameters	SI Units	Field Units
Formation permeability (base), k_{sand}	$5.92 \times 10^{-18} \text{ m}^2$	$6.00 \times 10^{-3} \text{ md}$
Formation permeability (higher), k_{sand}	$2.96 \times 10^{-17} \text{ m}^2$	$3.00 \times 10^{-2} \text{ md}$
Formation permeability (lower), k_{sand}	$1.18 \times 10^{-18} \text{ m}^2$	$1.20 \times 10^{-3} \text{ md}$

such high levels (in comparison to the formation permeability) resulted in an infinite-conductivity conduit in the slot in all the cases. The observed difference in production rates at very early times was because of the drainage of the artificially created initial fluid saturation in the slot. As expected, this drainage was faster in the case with the higher slot permeability.

Sensitivity to the Formation Permeability. The expected production performance of the SD method in the tight-gas-reservoir, shale-gas-reservoir, and tight/shale-oil-reservoir system and how this performance compares with the performance of MSHF (the preferred completion method in these formations) has been discussed earlier. In all these studies, the MSHF treatment outperformed the SD method. The issue that has not been addressed is whether a change in the selected formation permeability can cause a change in the earlier-observed trend.

The tight-gas- and shale-gas-reservoir comparative studies that we conducted earlier served as base (reference) cases, and involved (a) a comparison of production from the SD method with that from MSHF and (b) a comparison of production from the standard MSHF system to that from the system in which the SD technique was combined with MSHF. In this study, we investigated the sensitivity of production to changes in the formation

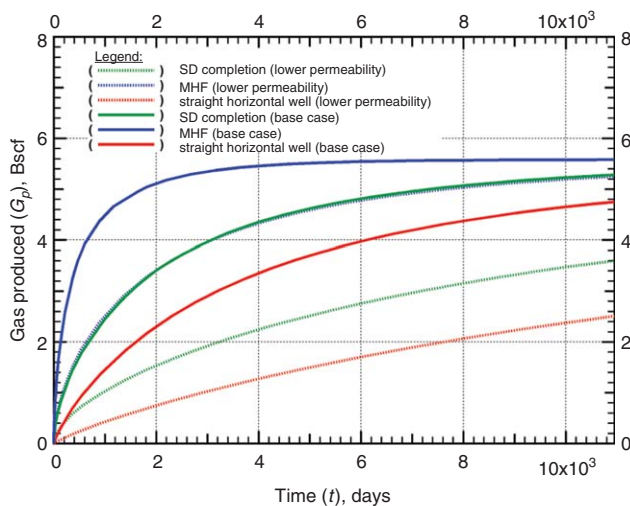


Fig. 25—Cumulative production from the SD (Geometry C), MSHF (Geometry E), and straight-well (Geometry A) cases when a lower formation permeability was used to simulate production in the tight-gas-formation system.

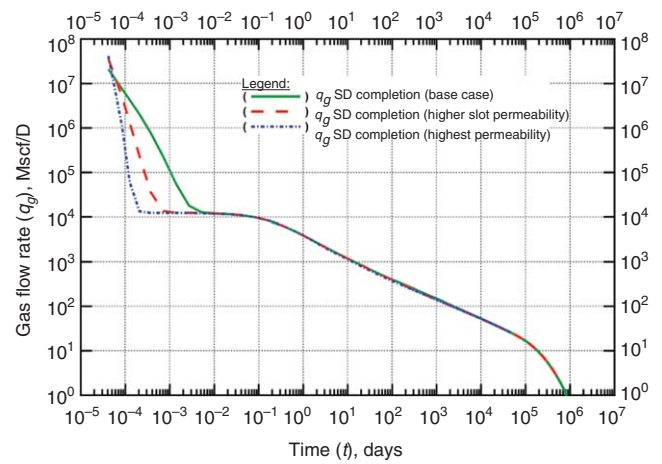


Fig. 24—Simulation results showing that the production rates from the SD method are insensitive to the slot-permeability values considered in the sensitivity study.

permeability. The values that we used for the formation permeability are listed in Table 6.

Figs. 25 and 26 show the cumulative production obtained when the simulations in the first comparative study (between the SD system and the MSHF system) were rerun with the lower and higher values of the formation permeability. From these plots, we determine that, though the magnitude of the formation-permeability effect varies, the qualitative deduction stays the same—the MSHF completion always outperforms the SD completion across the range of formation-permeability values considered in the tight-gas-formation system studied.

Similarly, we evaluated the sensitivity of production to the formation permeability in the second comparative study (between the standard MSHF system and the system in which the SD technique was combined with MSHF). The simulations were also reconducted with the lower and higher values of the formation permeability. As in the base cases, the production advantage resulting from adding the SD completion to an MSHF system (the combination case) was marginal. As a result, a detailed economic analysis would need to be carried out to determine whether the additional cost required to combine the SD method with hydraulic

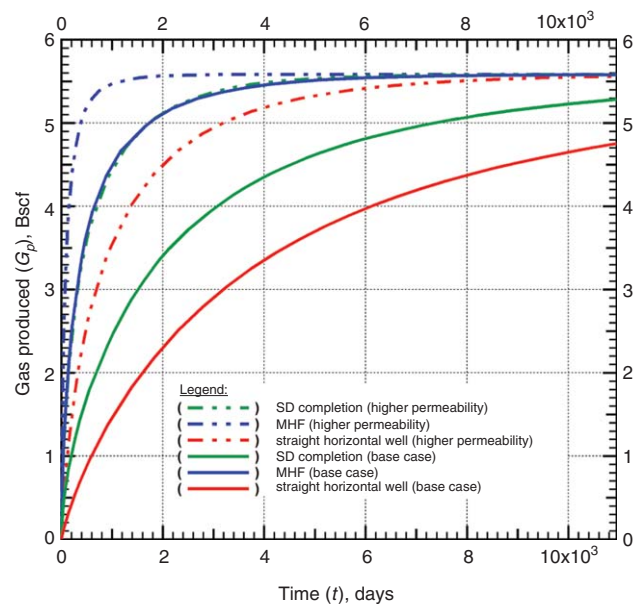


Fig. 26—Cumulative production from the SD (Geometry C), MSHF (Geometry E), and straight-well (Geometry A) cases when a higher formation permeability was used to simulate production in the tight-gas-formation system.

TABLE 7—SHALE GAS: FORMATION-PERMEABILITY SENSITIVITY PARAMETERS

Parameters	SI Units	Field Units
Formation permeability (base), k_{shale}	$7.402 \times 10^{-20} \text{ m}^2$	$7.5 \times 10^{-5} \text{ md}$
Formation permeability (higher), k_{shale}	$7.402 \times 10^{-19} \text{ m}^2$	$7.5 \times 10^{-4} \text{ md}$
Formation permeability (lower), k_{shale}	$7.402 \times 10^{-21} \text{ m}^2$	$7.5 \times 10^{-6} \text{ md}$

fracturing would be justified. This was the conclusion made in the base case and, as such, the qualitative inferences made from the base-case study remained unchanged for these tested values of the formation permeability.

In the shale-gas-system part of this sensitivity study, the case formation permeability was increased and decreased by a factor of 10 relative to that in the base case, as can be seen in **Table 7**.

The trends observed in the results and the conclusions drawn from this sensitivity study in the shale-gas formation were similar to those in the tight-gas-formation case. The results showed that the MSHF completion always outperformed the SD completion across the range of formation-permeability values considered in the shale-gas system, and that a detailed economic analysis would need to be carried out to determine whether combining the SD method with MSHF would be economically viable.

Sensitivity to the Fracture Permeability/Conductivity. The final sensitivity study that we conducted focused on the fracture permeability. The reservoir/completion parameters used to model

the MSHF treatment in the base case result in a dimensionless fracture conductivity (C_{fD}) of 20,280. This means that the fractures can be considered to have practically infinite conductivities. This might not always be true under field conditions—thus, the motivation for this sensitivity study. In this set of simulations, we used the shale-gas-reservoir parameters and four C_{fD} values that were lower (see **Table 8**) than those in the reference case.

The resulting rate performance in all cases is shown in **Fig. 27**, which includes, for comparison, the rates corresponding to the base case and the SD completion. As expected, the lower the fracture conductivity, the longer it takes for the formation to transition from the transient-flow regime into the linear-flow regime. In Case 5, the fracture permeability is so low that no linear-flow period was evident during the entire reservoir depletion. The cumulative-production curves corresponding to all the cases are also shown in **Fig. 28**. An interesting observation is that, in the rate and cumulative-production plots presented in Figs. 27 and 28, respectively, the curves for the first two cases coincided. This is because the fractures in those cases ($C_{fD} = 20,280$ and $2,028$) were practically infinitely conductive. As the fracture conductivity is reduced in the subsequent cases, the decline in the cumulative production after 100 years becomes more pronounced. In addition, the cumulative production from the SD completion only surpasses that corresponding to the MSHF case with the lowest conductivity. The obvious conclusion is that, with the exception of cases with very low fracture conductivity (and not considering other mitigating circumstances unrelated to the reservoir properties—see earlier discussion), the MSHF completion would still be the preferred option.

Conclusions

We analyzed the production-enhancement potential of the SD-completion method in three low-/ultralow-permeability formations—

TABLE 8—SHALE-GAS-RESERVOIR FRACTURE-CONDUCTIVITY SENSITIVITY PARAMETERS

Case	k_{frac} , md	k_{frac} , m ²	C_f , mm-m ²	C_f , md-ft	C_{fD}
Base	5.07×10^4	5.0×10^{-11}	1.5×10^{-10}	4.99×10^2	2.028×10^4
2	5.07×10^3	5.0×10^{-12}	1.5×10^{-11}	4.99×10^1	2.028×10^3
3	5.07×10^2	5.0×10^{-13}	1.5×10^{-12}	4.99×10^0	2.028×10^2
4	5.07×10^1	5.0×10^{-14}	1.5×10^{-13}	4.99×10^{-1}	2.028×10^1
5	5.07×10^0	5.0×10^{-15}	1.5×10^{-14}	4.99×10^{-2}	2.028×10^0

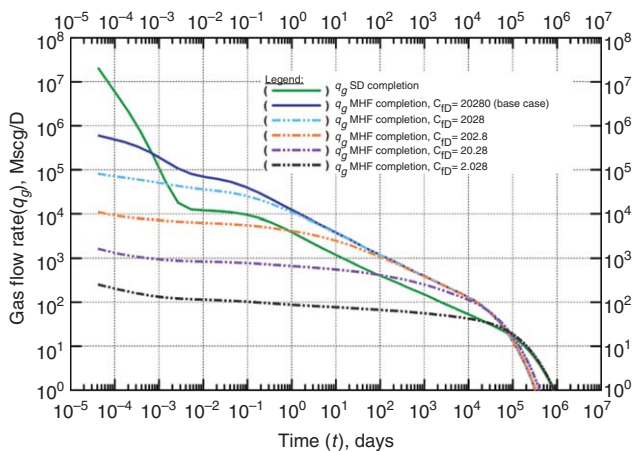


Fig. 27—Production from the MSHF systems with varying fracture conductivities compared with production from the SD completion method in the shale-gas reservoir studied.

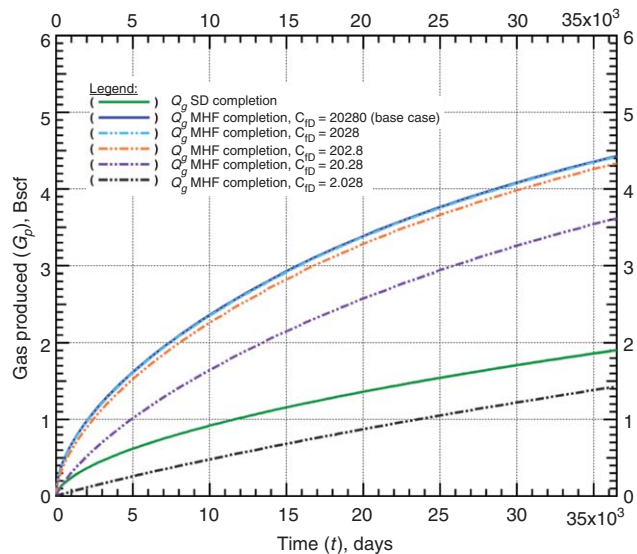


Fig. 28—Cumulative production from the different MSHF systems with varying fracture conductivities compared with the cumulative production from the SD-completion method in the shale-gas reservoir studied.

namely, tight gas reservoir, shale-gas reservoir, and tight/shale-oil reservoir. To this end, we developed six reservoir/completion mesh systems with Voronoi-gridding schemes. From this study, we reached the following conclusions:

- The ESD approach (which involves a much simpler discretization effort than a full representation of the complex SD geometry) can model production from the SD completion accurately and can be used in future studies.
- Nonreservoir issues and parameters notwithstanding, the MSHF treatment offers a clear and consistent advantage over the SD technique. Although an SD completion enhances production over the unstimulated case, it is consistently outperformed by the MSHF treatment, with the exception of cases of very low fracture permeability.
- In certain cases, promising improvements (over the case of standard treatment) in overall production can be attained when the MSHF was combined with the SD completion; a detailed economic analysis would be required to assess if the observed production boost would justify the extra cost to be incurred from combining the SD method with MSHF.
- There may exist cases—for example, the lack of adequate water volumes for hydraulic fracturing, or very high irreducible water saturation that leads to adverse relative permeability conditions and production performance—in which the low-cost SD method may make production feasible from an otherwise challenging (if not inaccessible) resource.

Nomenclature

C_f	= fracture conductivity, md-ft
C_{FD}	= dimensionless fracture conductivity
d_f	= fracture spacing, ft
h	= reservoir thickness, ft
k_f	= fracture permeability, md
k_{sand}	= matrix permeability, md
k_{shale}	= matrix permeability, md
k_{slot}	= slot permeability, md
L_w	= horizontal-well length, ft
p	= pressure, psi
p_i	= initial reservoir pressure, psi
p_{wf}	= wellbore flowing pressure, psi
q	= rate, B/D or Mscf/D
r_w	= wellbore radius, ft
t	= time, days
T	= temperature, °C or °F
w	= reservoir width, ft
w_f	= fracture width, in.
w_{slot}	= slot width, in.
x_f	= fracture half-length, ft
ϕ	= matrix porosity, fraction
ϕ_{frac}	= fracture porosity, fraction

Acknowledgements

This work was supported by RPSEA (Contract No. 08122-45) through the Ultra-Deepwater and Unconventional Natural Gas and Other Petroleum Resources Research and Development Program as authorized by the US Energy Policy Act (EPA) of 2005.

References

Bartberger, C.E., Dyman, T.S., and Condon, S.M. 2002. *Is There a Basin-Centered Gas Accumulation in Cotton Valley Group Sandstones, Gulf Coast Basin, U.S.A.?* <http://geology.cr.usgs.gov/pub/bulletins/b2184-d/> Accessed 2011-06-01.

Boleneus, D. 2010. *Estimate of Bakken Oil Resource*. McKenzie County, North Dakota USA: Bakken Resources Inc.

Carter, E.E. 2009. *Novel Concepts for Unconventional Gas Development of Gas Resources in Gas Shales, Tight Sands, and Coalbeds*. RPSEA 07122-7. http://www.rpsea.org/attachments/contentmanagers/2979/07122-07_Final_Report_P.pdf Accessed 2011-06-01.

Dyman, T.S. and Condon, S.M. 2006. Assessment of Undiscovered Conventional Oil and Gas Resources—Upper Jurassic–Lower Cretaceous Cotton Valley Group, Jurassic Smackover Interior Salt Basins Total Petroleum System, in the East Texas Basin and Louisiana-Mississippi Salt Basins Provinces. *US Geological Survey Digital Data Series DDS-69-E*.

Flannery, J. and Kraus, J. 2006. Integrated Analysis of the Bakken Petroleum System, US Williston Basin. Paper presented at the AAPG Annual Convention, Houston, Texas, 10–12 April.

Freeman, C.M. 2010. *Study of Flow Regimes in Multiply-Fractured Horizontal Wells in Tight Gas and Shale Gas Reservoir Systems*. MS thesis, Texas A&M University (May 2010).

GTI. 2001. “*Tight Gas Resource Map of the United States*”. In. Des Plaines, IL: Gas Technology Institute. GTI-01/0114

Halliburton. 2008a. *The Marcellus Shale*. http://www.halliburton.com/public/solutions/contents/Shale/related_docs/Marcellus.pdf Accessed 2011-06-01.

Halliburton. 2008b. U.S. Shale Gas: An Unconventional Resource. *Unconventional Challenges*. http://www.halliburton.com/public/solutions/contents/shale/related_docs/H063771.pdf Accessed 2011-06-01.

Heck, T.J., Lefever, R.D., Fischer, D.W. et al. 2012. *Overview of the Petroleum Geology of the North Dakota Williston Basin*. <https://www.dmr.nd.gov/ndgs/Resources/WBPetroleumnew.asp>. Accessed 2012-03-06.

Moridis, G.J., Blasingame, T.A., and Freeman, C.M. 2010. Analysis of Mechanisms of Flow in Fractured Tight-Gas and Shale-Gas Reservoirs. Paper SPE 139250 presented at the SPE Latin American and Caribbean Petroleum Engineering Conference, Lima, Peru, 1–3 December. <http://dx.doi.org/10.2118/139250-MS>.

Naik, G.C. 2005. *Tight Gas Reservoirs—An Unconventional Natural Energy Source for the Future*. 2011. http://www.pinedaleonline.com/socioeconomic/pdfs/tight_gas.pdf Accessed 2011-04-10.

Oduowo, T. 2012. *Numerical Simulation Study to Investigate Expected Productivity Improvement Using the “Slot-Drill” Completion*, Texas A&M University.

Olorode, O.M. 2011. *Numerical Modeling of Fractured Shale-Gas and Tight-Gas Reservoirs Using Unstructured Grids*. MS thesis, Texas A&M University (December 2011).

Rycroft, C.H. 2007. *Multiscale Modeling in Granular Flow*. PhD dissertation, Massachusetts Institute of Technology (September 2007).

Soeder, D.J. 1988. Porosity and Permeability of Eastern Devonian Gas Shale. *SPE Form Eval* 3 (1): 116–124. <http://dx.doi.org/10.2118/15213-PA>.

US Department of Energy. 2009. *Modern Shale Gas Development in the United States: A Primer*, by Gwpc. Doc. DE-FG26-04NT15455, pt. Oklahoma City: US Department of Energy.

Zagorski, W.A., Bowman, D.C., Emery, M. et al. 2011. An Overview of Some Key Factors Controlling Well Productivity in Core Areas of the Appalachian Basin Marcellus Shale Play. Paper presented at the AAPG Annual Convention and Exhibition, Houston, Texas, 10–13 April. AAPG Search and Discovery Article #110147.

Toluwanimi Oduowo is a petroleum engineer at DeGolyer & MacNaughton. His interests include numerical reservoir simulation, history matching, and production-data analysis. Oduowo holds an MS degree in petroleum engineering from Texas A&M University and a BS degree in petroleum engineering from the University of Ibadan.

George Moridis has been a staff scientist in the Earth Sciences Division of Lawrence Berkeley National Laboratory (LBNL) since 1991, where he is the Head of the Hydrocarbon Resource Program, is in charge of the LBNL research programs on unconventional resources (hydrates, tight/shale gas, and oil), and leads the development of the new generation of LBNL simulation codes. Moridis is a visiting professor in the Petroleum Engineering Department at Texas A&M University, and in the Guangzhou Center for Gas Hydrate Research of the Chinese Academy of Sciences; he is also an adjunct professor in the Chemical Engineering Department at the Colorado School of Mines, and in the Petroleum and Natural Gas Engineering Department of the Middle East Technical University, Ankara, Turkey. He holds MS and PhD degrees from Texas A&M University and BS and ME degrees in chemical engineering from the National Technical University of Athens, Greece. Moridis is the

author or coauthor of more than 70 papers in peer-reviewed journals and more than 180 LBNL reports, paper presentations, and book articles; and he holds three patents. He was an SPE Distinguished Lecturer for 2009–2010, and was elected an SPE Distinguished Member in 2010. Moridis is the recipient of a 2011 Secretarial Honor Award, the highest nonmonetary award of the US Department of Energy. He is on the editorial board of three journals, is an associate editor of four scientific journals, and is a reviewer for 26 scientific publications.

Tom Blasingame is a professor and is the holder of the Robert L. Whiting Professorship in the Department of Petroleum Engineering at Texas A&M University in College Station, Texas. He holds BS, MS, and PhD degrees from Texas A&M University — all in petroleum engineering. In teaching and research activities, Blasingame focuses on petrophysics, conventional- and unconventional-reservoir engineering, analysis/interpretation of well performance, and technical mathematics. He is an SPE Distinguished Member and a recipient of the 2005 SPE Distinguished Service Award, the 2006 SPE Lester C. Uren Award (for technology contributions before age 45), the 2012 SPE Anthony Lucas Medal (SPE's pre-eminent technical award), and

the 2013 SPE DeGolyer Distinguished Service Medal, and he has served as an SPE Distinguished Lecturer (2005–2006). Blasingame has prepared more than 120 technical articles, and he has chaired numerous technical committees and technical meetings. Blasingame also served as Assistant Department Head (Graduate Programs) for the Department of Petroleum Engineering at Texas A&M University from 1997 to 2003, and he has been recognized with several teaching and service awards from Texas A&M University.

Olufemi Olorode is a petroleum engineer at Afren Resources. His interests include numerical reservoir simulation, history matching, uncertainty analysis, and probabilistic production forecasting. Olorode holds an MS degree in petroleum engineering from Texas A&M University and a BS degree in petroleum engineering from the University of Ibadan.

C. Matt Freeman is a petroleum engineer at Hilcorp Energy Company. His interests include numerical reservoir simulation, simulation-mesh generation, and unconventional oil and gas. Freeman holds a BS degree in chemical engineering and MS and PhD degrees in petroleum engineering from Texas A&M University.